



HAL
open science

Future urban heat island influence on precipitation

Birthe M. Steensen, Louis Marelle, Ø. Hodnebrog, G. Myhre

► **To cite this version:**

Birthe M. Steensen, Louis Marelle, Ø. Hodnebrog, G. Myhre. Future urban heat island influence on precipitation. *Climate Dynamics*, 2022, 58, pp.3393-3403. 10.1007/s00382-021-06105-z . insu-03706365

HAL Id: insu-03706365

<https://insu.hal.science/insu-03706365>

Submitted on 28 Jun 2022

HAL is a multi-disciplinary open access archive for the deposit and dissemination of scientific research documents, whether they are published or not. The documents may come from teaching and research institutions in France or abroad, or from public or private research centers.

L'archive ouverte pluridisciplinaire **HAL**, est destinée au dépôt et à la diffusion de documents scientifiques de niveau recherche, publiés ou non, émanant des établissements d'enseignement et de recherche français ou étrangers, des laboratoires publics ou privés.



Distributed under a Creative Commons Attribution 4.0 International License



Future urban heat island influence on precipitation

B. M. Steensen¹ · L. Marelle^{1,2} · Ø. Hodnebrog¹ · G. Myhre¹

Received: 7 December 2020 / Accepted: 9 December 2021 / Published online: 23 January 2022
© The Author(s) 2021

Abstract

Urbanization and global warming are two of the major human impacts on the environment. The Urban Heat Island (UHI) effect can change precipitation patterns. Global warming also leads to changes in precipitation and especially an increase in intensity and frequency of extreme precipitation. With urbanization expected to grow in the future, the role of UHI in a warmer climate is an important research question. We present results from 20-year long regional convection-permitting model simulations that include the UHI effect, run for historical and future climates for two megacities, Paris and Shanghai. In the warmer future climate, urban-induced precipitation is found to decrease compared to the historical climate, for both mean and extreme precipitation, with large uncertainties due to natural variability. The mean precipitation increase due to UHI in Paris is $2.2 \pm 1.4\%$ and $1.8 \pm 1.3\%$ for historical and future conditions, respectively. Shanghai has slightly weaker mean precipitation change than Paris at present and no change in the future. The future reduction of the urban effect is found to be caused by a decrease in summer precipitation for both cities. Interannual variability in precipitation due to UHI is larger for Shanghai than Paris. The UHI effect on extreme precipitation is also reduced in the future climate and the area with precipitation increase is more concentrated. The general increase in extreme precipitation due to global warming, in combination with the precipitation redistribution due to UHI, underline the importance for future urban planning to mitigate damage caused by extreme precipitation events.

Keywords Precipitation · Global warming · Urbanization · Extreme events

1 Introduction

Urban Heat Islands (UHI) are formed when cities have higher temperatures than surrounding rural areas (Oke 1982; Arnfield 2003). Compared to rural vegetated areas, urban surfaces have different thermal properties such as lower albedo, less water available for evaporative cooling as well as higher potential for heat storage (Taha 1997). Excess anthropogenic heat emission (AHE) caused by human activity such as fuel combustion, e.g. from transport and air conditioning, is also an important contribution to UHI (Ichinose et al. 1999; Dong et al. 2017).

UHI produced by large urban areas can impact precipitation by enhancing low-level convergence, due to both

increase in surface roughness and destabilization of the boundary layer (Theilen et al. 2000; Bornstein and Lin 2000; Shepherd and Burian 2003). Regional numerical modelling at convection-permitting scales improves our understanding of these processes (Shepherd 2005; Shepherd et al. 2010). Wan et al. (2013) and Zhong et al. (2017) studied UHI effects in Shanghai and other urban areas in the Yangtze River Delta by changing the land use in convection-permitting numerical models. Wan et al. (2013) studied one event, while Zhong et al. (2017) ran the model over 5 years, both studies found that the UHI alters the circulation patterns and cause an increase in precipitation. This effect is also found in studies over other regions (Argüeso et al. 2016; Liu and Niyogi 2019). Zhang et al. (2018) found that the urbanization of Houston even had a substantial effect with increase in extreme precipitation during hurricane Harvey. Marelle et al. (2020) studies UHI effects in four mega cities over long enough time scales (10 and 20 years) to investigate the climatic impact on extreme precipitation on a convection-permitting scale by changing land cover and using high resolution AHE. The study finds that UHI increases the intensity

✉ B. M. Steensen
birthe.steensen@cicero.oslo.no

¹ CICERO Center for International Climate Research,
0318 Oslo, Norway

² Present Address: Université de Grenoble Alpes, CNRS, IRD,
IGE, Grenoble, France

and especially frequency of extreme precipitation over urban areas.

With global warming the hydrological cycle amplifies and causes changes in mean and extreme precipitation that differ globally (Douville et al. 2021; Pfahl et al. 2017; Hodnebrog et al. 2019). This leads to an increase in intensity (Fischer and Knutti 2016) and frequency of extreme precipitation (Myhre et al. 2019). The number of events that cause flooding or damages is therefore expected to occur more frequently in a warmer climate, and this should be accounted for in future adaptation management. In addition, urbanization is expected to continue to grow, 55% of the world's population lived in urban areas in 2018 and this is projected to reach 68% by 2050 (WUP 2018). As more people live in impenetrable urban areas, in a warming climate with more extreme precipitation, the added effect of UHI on precipitation is therefore of high importance for future urban planning.

Studies have shown that increasing urbanization leads to a larger heat storage and larger nighttime temperature difference between urban and rural areas, and especially nighttime UHI is correlated with urban population and less dependent on the climate zone of the city (Zhao et al. 2014; Imran et al. 2019). Daytime UHI is however more dependent on the climate the city is situated in as well as precipitation due to the limits of evaporative cooling in urban areas (Manoli et al. 2019). Scott et al. (2018) studied 54 United States cities for 2000–2015 and found that over interannual timescales, the UHI does not change with a warmer climate. Hamdi et al. (2015) used model simulations for Paris and Brussels to show that with future climate change, the biggest difference in UHI intensity is seen in nighttime temperatures during winter, caused by less wind. They also found a decrease in daytime UHI during summer, caused by drying soil outside of the urban areas. As climate change leads to different precipitation patterns, the future UHI effects on precipitation can be different than under current conditions. A model study by Georgescu et al. (2021) over the continental United States found that future urban expansion can both suppress or enhance extreme precipitation depending on season and location. Zhang et al. (2009) found that precipitation over a growing Beijing had decreased due to less evaporation and results presented in Trusilova et al. (2008) show a reduction in precipitation over urban areas in central Europe explained by less water availability in the extensive urban areas. In this study the UHI effect on precipitation will be explored by using regional numerical modelling at convection-permitting scales for simulations that include the urban effects and parallel simulations without the urban landcover for current climate and a future projection. The cities studies include Paris, where future projections indicate a small reduction in summer precipitation, and Shanghai, which is affected by the Asian monsoon that is projected to intensify.

Here, we use the same regional model setup as Marelle et al. (2020) for historical and future climate projections. To get a strong signal for global warming, a high emission scenario is chosen for the future projections. First, results are shown for mean and extreme precipitation indices for the UHI effect in historical and future conditions. Thereafter, the changes in extreme precipitation from historical to future conditions are investigated further.

2 Methods

Model simulations are performed with the Weather Research and Forecasting model (WRF) version 3.9.1 (Skamarock and Klemp 2008) at a convection-permitting horizontal resolution of 3 km. This inner 3 km domain is 483 km × 483 km wide and is nested in an intermediate 15 km domain which again is nested in an outer 45 km grid. Temperature, horizontal winds and geopotential height are spectrally nudged for the outermost 45 km grid. There are 50 vertical levels with a model top at 50 hPa. The WRF model setup in terms of physics schemes and parameterizations is given in Table S1.

The initial and 6-hourly boundary conditions to WRF are taken from a coupled atmosphere-ocean model simulation with the National Center for Atmospheric Research (NCAR) Community Earth System Model (CESM 1.0.4) (Gent et al. 2011), and are the same as in Hodnebrog et al. (2019). Sea-surface temperatures are also provided by the CESM results. The CESM is run using the CAM4 atmosphere module (Neale et al. 2010) with a 1.9 × 2.5 horizontal resolution and 26 vertical levels, with the CLM4 land module (Lawrence et al. 2011), a full ocean model (Danabasoglu et al. 2012) that is based on the Parallel Ocean Program 2 (Smith et al. 2010) and with the CICE4 sea-ice model (Hunke and Lipscomb 2008). Soil moisture and temperature to WRF are interpolated from the 15 CLM4 soil levels to four soil levels used by WRF. The CESM model run is from 1850 to 2100 with the high emission Representative Concentration Pathway 8.5 (RCP8.5) (van Vuuren et al. 2011).

WRF is run over the two megacities Paris and Shanghai for the years 1986–2005 representing historical conditions, and 2081–2100 representing future conditions, with different urban settings in the inner 3 km domain as described in Marelle et al. (2020). Land cover is obtained from the Moderate Resolution Imaging Spectroradiometer (MODIS) satellite instruments (Lu et al. 2008). For the 'urban' simulations, a global dataset with AHE estimations with a spatial resolution of 30-arc seconds is provided by Dong et al. (2017). The emissions dataset is estimated for the year 2013 and is given on monthly basis with a 1 hourly diurnal resolution. For the 'nourban' simulations, the urban land use for each city is replaced by the main land cover surrounding the city,

mostly cropland and the AHE is set to 0. As urbanization is expected to continue to increase (WUP 2018), sensitivity simulations with a larger and warmer city called ‘exurban’ is run over the last 10 years for the future conditions (2091–2100). During the last 30 years up to present, Paris and Shanghai have grown at different speeds (WUP 2018) and continued urbanization is projected to be less for Europe than China. Assumptions made in the ‘exurban’ simulations about increase in urban land use and AHE for the two cities are therefore different (see exurban extent in Fig. S1 vs. urban extent in Fig. 1). For Paris, the urban grid cells are expanded by ~ 60% around the city, and mean AHE over all the urban grid cells is increased with 50%. For Shanghai, the outer city is extended over Yangtze estuary, with AHE in this extended part set at the same values as in the original outer grid cells of the city, as well as an increase in AHE with 50% for the original urban grid cells. These changes are similar to the observed urban changes over the last 30 years for both cities (WUP 2018). A secondary use of the exurban simulations is to check the effects of only the increase in AHE over the original urban grid called ‘exahe’.

The effect of urbanization on extreme precipitation is found by studying the percent increase between the 99th and 99.72nd percentile thresholds for both daily and hourly precipitation for the whole year. The 99th percentile corresponds to the 1% most extreme days or hours, and the 99.72nd percentile corresponds to 1 day or 24 h per 365 days. The percent increase in total amount of precipitation above the percentiles is also calculated and called R99p_all

and R99.72p_all as in Myhre et al. (2019). These two latter statistics combine both the increase in intensity and frequency of extreme precipitation. In addition the percent increase in the day and hour of each year simulated with the maximum day and hourly precipitation (Rx1day and Rx1hour respectively) is studied.

3 Results

The UHI effect is calculated by the difference between simulations for urban and nurban. This UHI effect is calculated for historic and future conditions.

3.1 UHI effect on mean temperature and precipitation

Figure 1 show the annual mean impact of UHI on temperature and precipitation; both accumulated and yearly extreme precipitation for the two 20-year time periods are explored for Paris and Shanghai. The warming from UHI is up to 2.2 K in the city centers for Paris and Shanghai. Even though the temperature difference due to UHI shown for the two time periods is comparable, the historical conditions (1986–2005) UHI has a bigger impact on mean precipitation increase over the urban grid cells compared to end of the century conditions (2081–2100) for both cities. However, there is large natural variability connected to the effect of UHI on precipitation, the model results show that

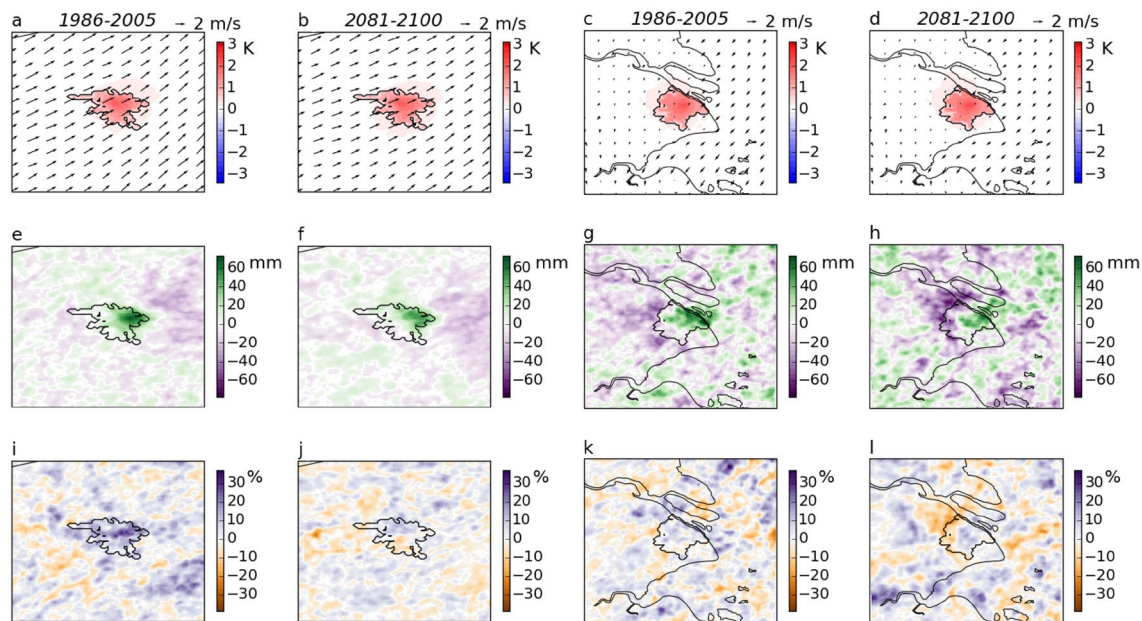


Fig. 1 Annual mean temperature difference and urban wind speed and direction (a–d), annual accumulated precipitation difference (e–h) and percent change for Rx1day (i–l) between the urban and

nurban simulations for Paris (left) and Shanghai (right) for the two 20-year simulations 1986–2005 and 2081–2100

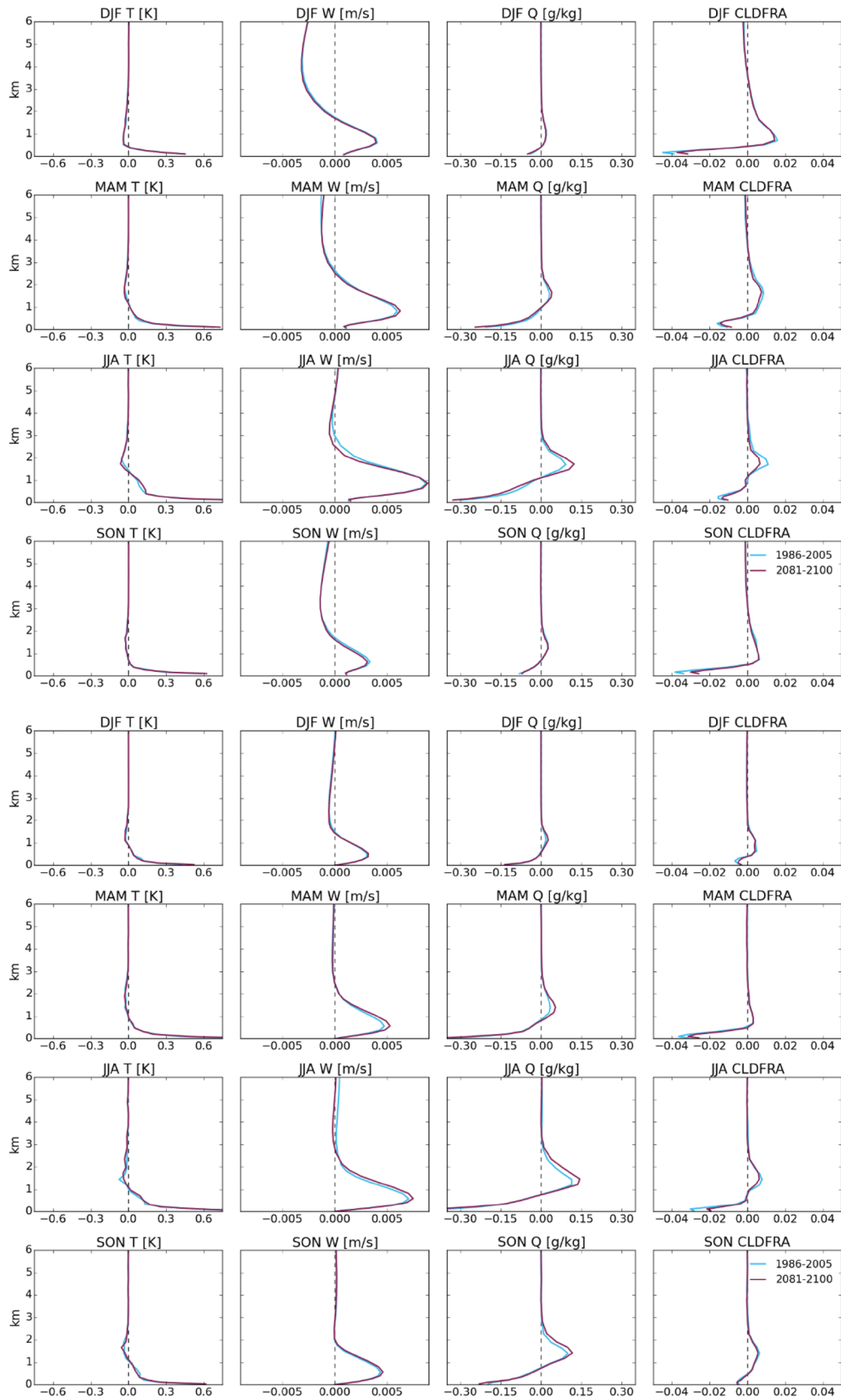


Fig. 2 Seasonal vertical profiles for Paris (top) and Shanghai (bottom) for temperature (T), vertical windspeed (w), water vapor mixing ratio (Q) and cloud fraction (CLDFRA) as a mean difference between the urban and nurban simulations, evaluated over the urban grid cells for the two 20 year periods 1986–2005 (blue) and 2081–2100 (burgundy). Height over ground shown on y-axis in km

mean increase over the Paris urban grid cells from 1986 to 2005 is 20.5 mm/year corresponding to a 2.2% increase, with an interannual variability of 13.4 mm (1.4%) calculated as standard deviation of the 20 years. For 2081–2100, the mean increase is 15.1 mm/year with an interannual variability of 10.1 mm, or 1.8% increase with a variability of 1.3%. For Shanghai the interannual variability is larger due to the city being affected by the monsoon and therefore have more convective precipitation. This causes the mean increase over the urban grid cells from 1986 to 2005 to be 15.9 mm/year or 1.6%, with an interannual variability of 26.4 mm (2.5%), and from 2081 to 2100 there is only a mean increase of 0.1 mm/year although the interannual variability is 47.8 mm (0.0% \pm 5.2%). Despite the large interannual variability, the increase in precipitation due to UHI over the urban grid cells is found to be statistically significant based on the Wilcoxon single-rank test ($p < 0.05$) except for the future (2081–2100) Shanghai simulations.

The Paris UHI effect on accumulated precipitation shows that for both time periods there is an increase on the north-east side, but with less precipitation difference for the end of century simulations. The UHI effect on accumulated precipitation for Shanghai also shows an increase over a region in the north-eastern side of the city, but this region becomes smaller from historical to future conditions, and the westerly regions with a reduction in precipitation become larger. For the sensitivity simulation (exurban) with a larger urban area and warmer Shanghai (Fig. S1d), this westerly region with precipitation reduction is even larger. This indicates that the UHI effect in Shanghai changes the precipitation pattern, and a warmer city intensifies this tendency. The UHI effect on accumulated precipitation shows relatively small differences when a larger urban area of Paris (exurban) was assumed instead of the current spatial extent of the city (Fig. S1c).

There is a clear increase over Paris for the annual maximum 1-day precipitation (Rx1day) in the historical conditions (over 20% in parts of the city), while end of the century results do not show a clear impact of the Paris UHI. In comparison, Shanghai does not show such a clear impact of UHI on Rx1day for either of the periods, although the pattern of change in Rx1day values is similar to the accumulated precipitation change pattern. When future urban expansion is considered (the exurban simulations) the Rx1day percent increase is similar to the original city with no real signal for Paris. For Shanghai,

there is a larger percent decrease in Rx1day to the west and a smaller increase to the east, also similar to the accumulated precipitation pattern. (Fig. S1e, f).

To further explore the change in UHI effect between historical conditions and a warmer climate the impact in different seasons is investigated. Figure 2 shows the seasonal UHI impact on temperature (T), vertical wind (w), water vapor mixing ratio (Q) and cloud fraction for Paris and Shanghai in the lowest 6 km above the urban grid cells. Even though the cities are situated in different climates, the UHI impact is similar over the seasons: Temperature increase close to ground leads to an increase in updrafts and a reduction in Q and cloud cover. Above 1000 m, the updraft causes an increase in Q and cloud fraction, leading to a small decrease in temperature in the altitude with enhanced cloud cover. The UHI effect is strongest during the summer months, and it is also during the summer months the two curves for historical and future conditions differ most. While the increase in Q over 1000 m is not as strong for historical as for future conditions, historical conditions show a stronger increase in cloud fraction (although stronger increase for Paris than for Shanghai).

To understand the effect of the UHI in historical and future climate, the change in climate between the two time periods studied is of interest. Figure S2 show the absolute values in the nurban simulations for historical and future condition. The variables (except omega as a substitute of w for updraft) for the global climate model from the grid point closest to the city center is also shown. Both models show that the increase in greenhouse gases leads to around two degrees warming in the profile and up to three degrees for Shanghai during the summer months. Although there is an increase in water vapor mixing ratio, the mean cloud fraction shows a decrease (with less clouds in the WRF model results compared to CAM4) in future compared to present day climate.

Figure S3 shows the same as Fig. 2 but includes the effect of the larger city area and future climate sensitivity (exurban) simulations. Profiles are calculated both as a mean over the original urban area to study just the increase in anthropogenic heat (exahe), and as a mean over all the expanded city grid cells (exurb). Urban expansion combined with global warming has the strongest impact on the profile of water vapor change (stronger reduction close to the ground and a stronger increase above 1000 m), especially during the summer months for both cities as well as fall for Shanghai. For Paris, however, there is no further increase in cloud fraction for the summer months due to urban expansion, and just a small increase during the rest of the year. For Shanghai, independent of the city area (both exahe and exurb) there is a small cloud fraction increase for summer and fall, even though the areas where they are evaluated are very different.

Figure 2 showed that the UHI effect is strongest during summer, both for surface temperature and in the vertical column. Figure 3 shows the seasonal mean 2-m temperature and accumulated precipitation difference for summer (JJA) and winter months (DJF) for Paris (spring (MAM) and fall (SON) are shown in Fig. S4). Even though the 2-m temperature difference is smaller for winter than the other seasons, this season show a clear influence of the UHI effect on precipitation in both historical and future simulations which is likely caused by the stronger mean wind in south westerly direction compared to the other seasons. Model results show more precipitation downwind on the east side of Paris, and a decrease further to the east outside of the city. For the summer months there is an increase in accumulated precipitation in the historical climate with a mean of 5.2 mm/(3 months) over the urban grid cells with interannual variations of 10.8 mm, while there is a decrease in a warmer climate with a mean of -3.3 mm/(3 months) over the urban grid cells with interannual variations of 9.4 mm. The decrease

during summer causes the lower annual mean urban-induced precipitation in the end of the century simulations compared to historical climate. The large interannual variation in the effect of UHI in summer precipitation is presumably a result of the variability of convective precipitation.

Due to the monsoon, there is a larger seasonal difference for Shanghai than for Paris. Most of the precipitation occurs in summer and fall (Fig. S5 show precipitation in winter, DJF and spring, MAM). Figure 4 shows that the distribution of accumulated precipitation difference between the urban and nourban simulations during summer is very similar to the annual precipitation difference, suggesting that this season accounts for large parts of the annual difference. Within the city of Shanghai, there is an area with an increase in precipitation due to the UHI effect on the east side and an area of decrease in precipitation further downwind in the westerly part, where the area of precipitation decrease is larger for the end of the century simulations than present day. Compared to Paris, the increase in mean precipitation

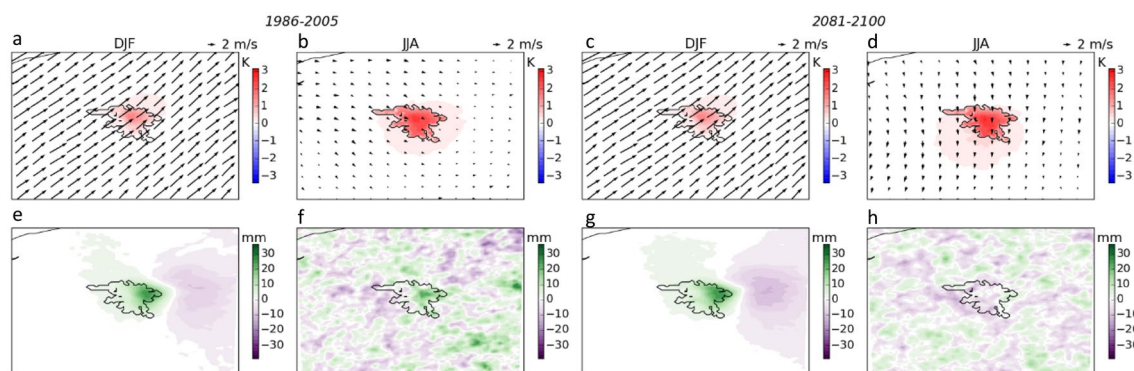


Fig. 3 Mean seasonal difference for temperature and seasonal accumulated precipitation for Paris in winter (DJF) and summer (JJA) for the two 20-year periods 1986–2005 and 2081–2100. For the upper plots, the mean seasonal wind speed in the urban simulation is also shown

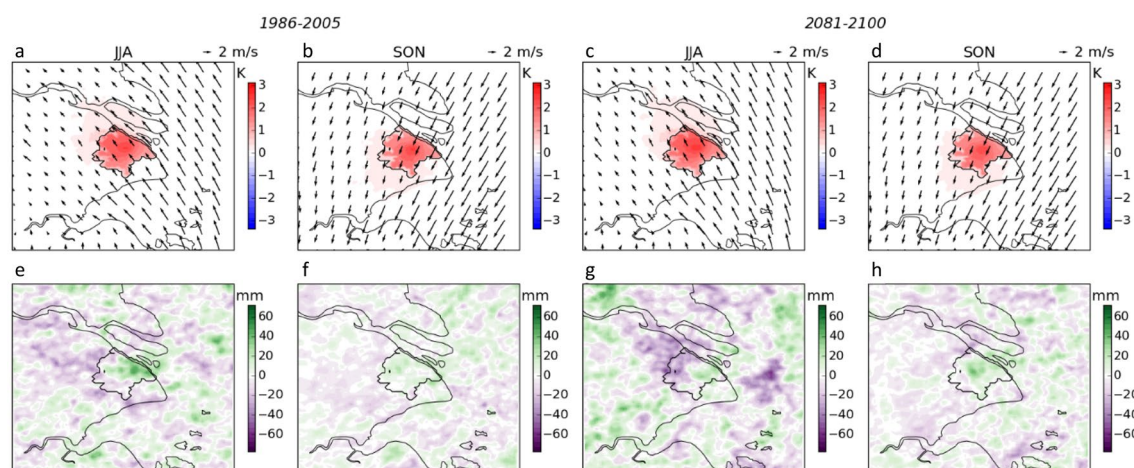


Fig. 4 Same as Fig. 3, but for Shanghai and for the summer (JJA) and fall (SON) seasons

occurs further to the upwind side of Shanghai. Similar to Paris, the decrease in annual mean precipitation in Shanghai is caused by the decrease in summer months with 7.2 mm/ (3 months) difference between the urban and nurban simulation for 1986–2005 and – 7.6 mm/(3 months) difference for and 2081–2100. Due to a large fraction of convective precipitation the interannual variations are large for these results as well with 23.8 mm and 44.3 mm, respectively.

3.2 UHI effect on extreme precipitation

The annual and seasonal mean maps in Figs. 1, 3 and 4 show that UHI contributes to increased precipitation in some parts of the cities and a decrease over other parts. Since precipitation can cause damages over a smaller area, extreme precipitation statistics are calculated both over all the urban grid cells and where the UHI effect has a positive annual mean difference (as shown in Fig. 1e–h), same methodology as used in Marelle et al. (2020). Marelle et al. (2020) showed that areas where mean precipitation increases within cities are also where extreme precipitation is the most influenced by UHI. Figure 5 shows the percent increase in annual mean and extreme precipitation due to the UHI as an average over all the urban grid cells and just the urban grid cells that has an increase in the yearly mean (pos urban). Also, the

percent increase for the 99th and 99.72nd percentiles (see Method section), and the change in amount of precipitation over these thresholds are shown. The percent increase in annual maximum 1-day precipitation (Rx1day) is calculated (equivalent to the maps shown in Figs. 1 and S1), as well as the annual maximum 1-h precipitation (Rx1hour). The interannual spread and standard deviation for the results are shown in Fig. S6.

The results show an increase in extreme precipitation due to UHI for historical conditions with a mean of 10.2% and 2.5% increase in Rx1day for all the urban grid cells of Paris and Shanghai, respectively, over the 20 years. The effect is larger for daily values compared to hourly for both cities (e.g. 8.3% and 2.2% for the corresponding 1-h annual extreme). For historical conditions, Paris has an overall stronger increase in extreme precipitation due to UHI compared to Shanghai, however for Shanghai there is a larger increase between the positive urban grid cells and all urban grid cells (from 2.5 to 3.7% increase in Rx1day). This shows that the areas that experience more mean precipitation due to UHI effects also have higher increase in extreme precipitation, and that the change in mean precipitation in Shanghai is more influenced by extreme precipitation events than that of Paris. Although the Rx1day is stated as an example in the text here, the overall tendencies is the same for the other

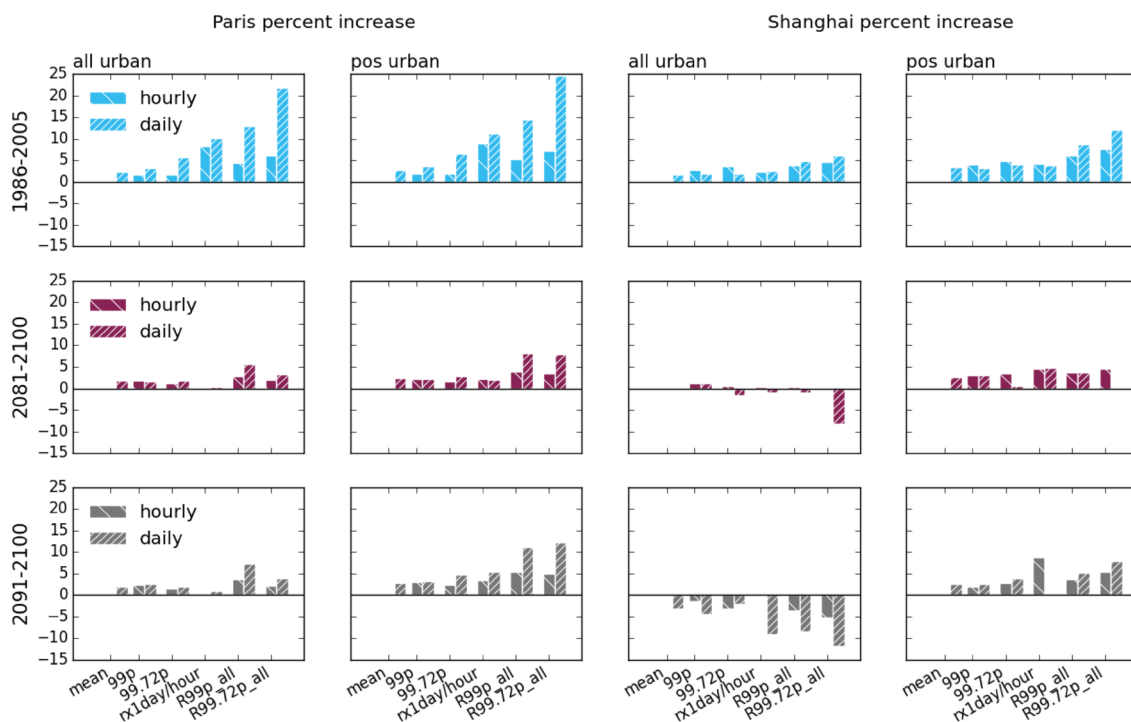


Fig. 5 Percent increase in mean precipitation and extreme precipitation indices for Paris (left) and Shanghai (right) for the two 20-year simulations 1986–2005 (top) and 2081–2100 (mid), and the sensitivity simulations with larger and warmer cities (exurban) over 10 years

2091–2100 (bottom). Results are calculated for all urban grid cells (“all urban”), and the urban grid cells where there is an increase in mean precipitation over the respective time periods (“pos urban”)

extreme precipitation statistics (based on percentiles) for historical conditions.

For future conditions, the UHI effects on extreme precipitation is lower than for historical conditions (down to a 0.3% increase in Rx1day for Paris and a negative effect of -0.9% for Shanghai), this is similar to what has been shown for mean precipitation. The difference between all urban grid cells and the grid cells with a positive mean precipitation change is larger for extreme precipitation in future conditions in Shanghai with 4.7% increase in Rx1day for “pos urban”, whereas Paris shows a smaller effect of 2% increase. A larger urban area and warmer Paris in the sensitivity simulation (exurban) increases the extreme precipitation compared to the standard future simulations, for example there is a 1% mean increase in Rx1day over all the exurban grid cells. The exurban sensitivity simulation for Shanghai shows a decrease over the whole city with -4.4% for the 99th percentile precipitation intensity (99p), however for the parts with a positive urban grid cells the effect of UHI on 99p is a 2.7% increase.

Compared to the results for the UHI effect for the 1986–2005 simulations, where there is an increase towards the more extreme statistics, the simulations representing 2081–2100 show a larger variation between the extreme precipitation indices for the same city, with some of the indices showing an increase and others showing no change. In Shanghai, extreme precipitation is more dependent on the monsoon and therefore more convective, and there the UHI effect even leads to a decrease in extreme precipitation intensity and amount when studying the 20 years combined but there are large interannual variations.

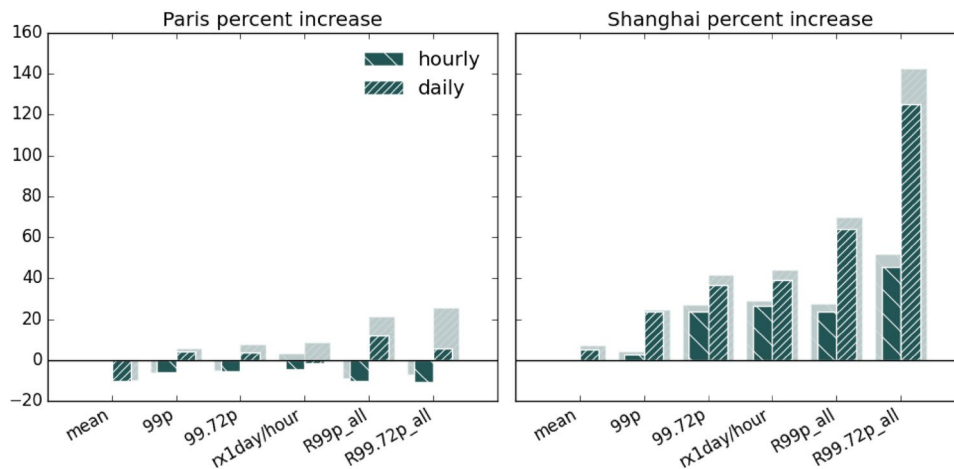
These large differences in UHI precipitation effects shown in Fig. S6, illustrate the need for long timeseries when studying the UHI effect on precipitation. There is

indeed also a larger spread for daily results compared to the hourly results that contains more data. The variations are also larger for the most extreme threshold and for future conditions. For most years, however, the results are centered around the values shown in Fig. 5 with outliers often to the more extreme events.

Even though the strength of the UHI intensity in temperature is similar in a warmer climate and historical conditions, the UHI effect on mean and extreme precipitation is weaker over the 20 years in the future. Figure 6 shows the same statistics as Fig. 5, but for percent increase from historical to future conditions over the urban grid cells (in both the urban and nourban simulations). For Paris there is around a 10% decrease in mean annual precipitation between 1980 and 2006 and 2081–2100, while there is a 5% increase for Shanghai. These results are similar to the median CMIP5 model results shown in the IPCC atlas (IPCC 2013), with a decrease in mean precipitation over central Europe and an increase in precipitation over Shanghai both with a RCP4.5 and a RCP8.5 scenario for the end of the century.

Even with a decrease in mean precipitation in Paris with global warming, extreme precipitation is found to increase in the 20-year long simulations, with a higher increase in the nourban simulation and daily data when comparing the indices. Hourly maximum precipitation due to UHI is found to decrease in both nourban and urban simulations compared to historical conditions. For Shanghai the model results show a strong increase in extreme precipitation without the UHI effect, with a stronger increase for the more extreme indices that also account for changes in frequency. Daily precipitation extremes increase more than hourly. These increases show that even though the urban-induced precipitation is shown to be lower in a warmer climate, a warmer climate leads to an increase in extreme precipitation.

Fig. 6 Same as Fig. 5, but with percent increase between the two 20-year time periods (1986–2005 and 2081–2100) for the urban simulations (green) and nourban simulations (shaded green)



4 Discussion

This study uses the same model setup as Marelle et al. (2020), but with boundary and initial conditions from a global climate model, limited to one realization of historical and future climate, while Marelle et al. (2020) use reanalysis data representing actual weather situations. Comparing the two studies shows that there is a higher impact of urbanization on mean precipitation and the yearly extreme here than in Marelle et al. (2020), but the spatial patterns are similar. Prevailing westerly winds in Central Europe and the Monsoon circulation are the main drivers of precipitation changes in both studies, and the differences seen between the studies can be caused by natural variability and the different time periods studied. As shown in both studies, because of the strong natural variability the results are very dependent on the time periods studied.

UHI effects increase precipitation by inducing updraft that initiate moist convection if the conditions are thermodynamic favorable (Han et al. 2014). Figure 2 shows that the UHI effect in Paris initiate the strongest updraft in summer, although mean horizontal wind (see Fig. 3) is weak during this season. For historical conditions there is an increase in mean precipitation during summer due to UHI, while in the future projections the UHI has a negative effect on the mean summer precipitation over Paris. There is also a reduced UHI effect on the annual mean and extreme precipitation in the future compared to historical conditions. Previous studies have found that this decrease in precipitation can be explained by a reduction in water availability in the urban areas (Trusilova et al. 2008; Zhang et al. 2009).

Compared to Paris, Shanghai show conditions that are more favorable for moist convection, and precipitation production in the urban simulations occurs more over the city than on the downwind side. This causes a decrease in precipitation over the rest of the city compared to the nourban simulations. In the future simulations, conditions are even more favorable and mean precipitation is increased right on the upwind side inside of the city, with a decrease further downwind for summer and fall mean wind directions. Additional expansion of the urban area of Shanghai in the exurban simulations show the same tendency with the area of increased precipitation displaced even further upwind, and a large area with precipitation decrease. The favorable conditions for convection can also be seen by the large increase in both mean and extreme precipitation for Shanghai with the future emission scenario. Even though the high emission scenario (RCP8.5) used in this study is uncertain, the trends in the results presented in this study is important for future city planning as RCP 4.5 also show an increase in precipitation over the Shanghai area (IPCC 2013).

The results found here suggest that a larger and warmer city increases the mean and extreme precipitation in the future, especially over smaller areas of the cities compared to if the city size and heat emission is kept at current levels. Increasing green areas is a common strategy to reduce the effect of UHI on temperature, as increased water available for evaporation reduces temperature but could also increase water available to be precipitated downwind of the city. With already increasing extreme precipitation due to global warming, and the flooding risks in the impenetrable urban areas, measures that reduce the UHI effect on precipitation is even more important.

5 Conclusions

We present results on the role of the UHI on mean and extreme precipitation, simulated by a convection-permitting regional model driven by a global climate model for a historical and a future scenario for Paris and Shanghai. The effect of UHI is studied by comparing model results that include the urban areas and anthropogenic heat to model results where the urban area is replaced with the surrounding land cover. Results show that the UHI leads to an updraft that increase moist convection with increase in water vapor and cloud fraction over the urban area. If conditions are favorable, this increased convection can cause an increase in precipitation downwind, causing a different precipitation distribution in the simulations that include urban effects compared to the nourban simulations.

Especially for historical conditions, the area with increased precipitation is located downwind of the prevailing wind directions, with a small decrease in the rest of the city. The UHI effect in Paris is stronger than in Shanghai for mean and extreme precipitation, both as a mean over all the grid cells and as a mean of the grid cells with a yearly positive mean increase in precipitation. Since precipitation in Shanghai is more convective, the results are more uncertain with a large interannual variability.

For future conditions, both cities have a reduced UHI effect on mean precipitation compared to historical conditions, with the largest reduction in summer precipitation. Sensitivity simulations with larger and warmer cities, due to assumptions of increased urbanization in the future, show the same result. Especially for Shanghai, conditions for moist convection are more favorable causing a stronger redistribution of the precipitation due to the UHI effects. Also, the area with increased precipitation is more concentrated in the downwind side of the city border in the future simulations, with a precipitation reduction further downwind compared to historical conditions. This leads to a negative mean precipitation over all the Shanghai urban grid cells, although flooding can still cause large damage

over the more concentrated area affected. The natural variability of convective and also extreme precipitation leads to large uncertainties, and the results are very dependent on the time period studied highlighting the need for long timescales.

Extreme precipitation events of short time-duration can lead to flooding, and with impenetrable urban surfaces, cities are more at risk. The urban effect on extreme hourly precipitation is less than the increase in daily extremes in both the historical and future simulations. For Paris, there is even a decrease in extreme hourly precipitation from historical to future climate, however for Shanghai the hourly extreme precipitation is found to increase although not as strongly as for the daily extremes. Even with a reduced effect of UHI on precipitation in the future model simulations compared to the historical, the model results also show that background extreme precipitation, due to global climate change, will increase in Paris and Shanghai, highlighting the need to account for changes in extreme precipitation in urban planning. This is important especially in the areas where the UHI redistribution of precipitation causes an increase.

Supplementary Information The online version contains supplementary material available at <https://doi.org/10.1007/s00382-021-06105-z>.

Author contributions All authors designed the study, contributed to the writing process and to the interpretation of the data. BMS and ØH performed simulations with WRF and CESM respectively. BMS and LM analyzed the data.

Funding The work has received support from the project SUPER (no. 250573) funded through the Research Council of Norway. The project SUPER has also received support from the insurance company If. The simulations were performed using the NN9188K project account and data was stored and shared on project accounts NS9188K on resources provided by UNINETT Sigma2—the National Infrastructure for High Performance Computing and Data Storage in Norway.

Availability of data and material The anthropogenic heat emission inventory is available online (http://www-old.ide.titech.ac.jp/~kandalab/ja/news/2016/AHE_release_20161212_files/AHE_release_20161212.htm).

Code availability The WRF 3.9.1 model is available at https://www2.mmm.ucar.edu/wrf/users/download/get_source.html. The CESM 1.0.4 model is available to download at <https://www.cesm.ucar.edu/models/cesm1.0/>.

Declarations

Conflicts of interest/Competing interests: Authors declare that they have no competing interest regarding this research.

Open Access This article is licensed under a Creative Commons Attribution 4.0 International License, which permits use, sharing, adaptation, distribution and reproduction in any medium or format, as long as you give appropriate credit to the original author(s) and the source, provide a link to the Creative Commons licence, and indicate if changes were made. The images or other third party material in this article are included in the article's Creative Commons licence, unless indicated otherwise in a credit line to the material. If material is not included in the article's Creative Commons licence and your intended use is not permitted by statutory regulation or exceeds the permitted use, you will need to obtain permission directly from the copyright holder. To view a copy of this licence, visit <http://creativecommons.org/licenses/by/4.0/>.

References

- Argüeso D, Di Luca A, Evans JP (2016) Precipitation over urban areas in the western Maritime Continent using a convection-permitting model. *Clim Dyn* 47(3–4):1143–1159
- Arnfield AJ (2003) Two decades of urban climate research: a review of turbulence, exchanges of energy and water, and the urban heat island. *Int J Climatol* 23(1):1–26
- Bornstein R, Lin Q (2000) Urban heat islands and summertime convective thunderstorms in Atlanta: three case studies. *Atmos Environ* 34(3):507–516
- Danabasoglu G, Bates SC, Briegleb BP, Jayne SR, Jochum M, Large WG, Peacock S, Yeager SG (2012) The CCSM4 ocean component. *J Clim* 25(5):1361–1389
- Dong Y, Varquez ACG, Kanda M (2017) Global anthropogenic heat flux database with high spatial resolution. *Atmos Environ* 150:276–294
- Douville H, Raghavan K, Renwick J, Allan RP, Arias PA, Barlow M, Cerezo-Mota R, Cherchi A, Gan TY, Gergis J, Jiang D, Khan A, Pokam Mba W, Rosenfeld D, Tierney J, Zolina O (2021) Water cycle changes. In: *Climate change 2021: the Physical Science Basis. Contribution of Working Group I to the Sixth Assessment Report of the Intergovernmental Panel on Climate Change*. Cambridge University Press. (in press)
- Fischer EM, Knutti R (2016) Observed heavy precipitation increase confirms theory and early models. *Nature Climate Change* 6(11):986–991
- Gent PR, Danabasoglu G, Donner LJ, Holland MM, Hunke EC, Jayne SR, Worley PH (2011) The community climate system model version 4. *J Clim* 24(19):4973–4991
- Georgescu M, Broadbent AM, Wang M, Krayenhoff ES, Moustaoui M (2021) Precipitation response to climate change and urban development over the continental United States. *Environ Res Lett* 16(4):044001. <https://doi.org/10.1088/1748-9326/abd8ac>
- Hamdi R, Giot O, De Troch R, Deckmyn A, Termonia P (2015) Future climate of Brussels and Paris for the 2050s under the A1B scenario. *Urban Clim* 12:160–182
- Han JY, Baik JJ, Lee H (2014) Urban impacts on precipitation. *Asia-Pac J Atmos Sci* 50(1):17–30
- Hodnebrog Ø, Marelle L, Alterskjær K, Wood RR, Ludwig R, Fischer EM, Myhre G (2019) Intensification of summer precipitation with shorter time-scales in Europe. *Environ Res Lett* 14(12):124050
- Hunke EC, Lipscomb WH (2008) CICE: the Los Alamos Sea Ice Model Documentation and Software User's Manual Version 4.0, LA-CC-06-012Rep
- Ichinose T, Shimodozono K, Hanaki K (1999) Impact of anthropogenic heat on urban climate in Tokyo. *Atmos Environ* 33(24–25):3897–3909
- Imran HM, Kala J, Ng AW, Muthukumaran S (2019) Impacts of future urban expansion on urban heat island effects during

- heatwave events in the city of Melbourne in southeast Australia. *Q J R Meteorol Soc* 145(723):2586–2602
- IPCC (2013) Annex I: atlas of global and regional climate projections. *Climate Change 2013: the physical science basis*. In: Stocker TF (ed) *Contribution of Working Group I to the Fifth Assessment Report of the Intergovernmental Panel on Climate Change*. Cambridge University Press, Cambridge, pp 1311–94
- Lawrence DM, Oleson KW, Flanner MG, Thornton PE, Swenson SC, Lawrence PJ, Bonan GB (2011) Parameterization improvements and functional and structural advances in version 4 of the Community Land Model. *J Adv Model Earth Syst* 3(1)
- Liu J, Niyogi D (2019) Meta-analysis of urbanization impact on rainfall modification. *Sci Rep* 9(1):1–14
- Lu D, Tian H, Zhou G, Ge H (2008) Regional mapping of human settlements in southeastern China with multisensor remotely sensed data. *Remote Sens Environ* 112:3668–3679
- Manoli G, Fatichi S, Schl pfer M, Yu K, Crowther TW, Meili N, Bou-Zeid E (2019) Magnitude of urban heat islands largely explained by climate and population. *Nature* 573(7772):55–60
- Marelle L, Myhre G, Steensen BM, Hodnebrog  , Alterskj r K, Sillmann J (2020) Urbanization in megacities increases the frequency of extreme precipitation events far more than their intensity. *Environ Res Lett* 15:124072
- Myhre G, Alterskj r K, Stjern CW, Hodnebrog  , Marelle L, Samset BH, Stohl A (2019) Frequency of extreme precipitation increases extensively with event rareness under global warming. *Sci Rep* 9(1):1–10
- Neale RB et al (2010) Description of the NCAR community atmosphere model (CAM 5.0), vol 1. NCAR Tech. Note NCAR/TN-486+ STR, pp 1–121
- Oke TR (1982) The energetic basis of the urban heat island. *Q J R Meteorol Soc* 108(455):1–24
- Pfahl S, O’Gorman PA, Fischer EM (2017) Understanding the regional pattern of projected future changes in extreme precipitation. *Nat Clim Change* 7(6):423–427
- Scott AA, Waugh DW, Zaitchik BF (2018) Reduced Urban Heat Island intensity under warmer conditions. *Environmental Research Letters* 13(6):064003
- Shepherd JM (2005) A review of current investigations of urban-induced rainfall and recommendations for the future. *Earth Interact* 9(12):1–27
- Shepherd JM, Burian SJ (2003) Detection of urban-induced rainfall anomalies in a major coastal city. *Earth Interact* 7(4):1–17
- Shepherd JM, Carter M, Manyin M, Messen D, Burian S (2010) The impact of urbanization on current and future coastal precipitation: a case study for Houston. *Environ Plant* 37(2):284–304
- Skamarock WC, Klemp JB (2008) A time-split nonhydrostatic atmospheric model for weather research and forecasting applications. *J Comput Phys* 227(7):3465–3485
- Smith R, Jones P, Briegleb B, Bryan F, Danabasoglu G, Dennis J, Hecht M (2010) The parallel ocean program (POP) reference manual: ocean component of the community climate system model (CCSM) and community earth system model (CESM). In: LAUR-01853, 141:1–140
- Taha H (1997) Urban climates and heat islands: albedo, evapotranspiration, and anthropogenic heat. *Energy Build* 25(2):99–103
- Thielen J, Wobrock W, Gadian A, Mestayer PG, Creutin JD (2000) The possible influence of urban surfaces on rainfall development: a sensitivity study in 2D in the meso- γ -scale. *Atmos Res* 54(1):15–39
- Trusilova K, Jung M, Churkina G, Karstens U, Heimann M, Claussen M (2008) Urbanization impacts on the climate in Europe: Numerical experiments by the PSU–NCAR Mesoscale Model (MM5). *J Appl Meteorol Climatol* 47(5):1442–1455
- Van Vuuren DP, Edmonds J, Kainuma M, Riahi K, Thomson A, Hibbard K, Masui T (2011) The representative concentration pathways: an overview. *Clim Change* 109(1–2):5
- Wan H, Zhong Z, Yang X, Li X (2013) Impact of city belt in Yangtze River Delta in China on a precipitation process in summer: A case study. *Atmos Res* 125:63–75
- WUP (2018) World Urbanization prospects: the 2018 revision. United Nations Department of Economic and Social Affairs/Population Division
- Zhang CL, Chen F, Miao SG, Li QC, Xia XA, Xuan CY (2009) Impacts of urban expansion and future green planting on summer precipitation in the Beijing metropolitan area. *J Geophys Res Atmos* 114:D2
- Zhang W, Villarini G, Vecchi GA, Smith JA (2018) Urbanization exacerbated the rainfall and flooding caused by hurricane Harvey in Houston. *Nature* 563(7731):384–388
- Zhao L, Lee X, Smith RB, Oleson K (2014) Strong contributions of local background climate to urban heat islands. *Nature* 511(7508):216–219
- Zhong S, Qian Y, Zhao C, Leung R, Wang H, Yang B, Liu D (2017) Urbanization-induced urban heat island and aerosol effects on climate extremes in the Yangtze River Delta region of China. *Atmos Chem Phys* 17(80):5439–5457

Publisher’s Note Springer Nature remains neutral with regard to jurisdictional claims in published maps and institutional affiliations.